Advances in Astronautics Science and Technology (2020) 3:125–131
https://doi.org/10.1007/s42423-020-00067-w

ORIGINAL PAPER

Radioluminescent Nuclear Battery Technology Development for Space Exploration

Zhiheng Xu[1] · Yunpeng Liu[1] · Xiaobin Tang[1]

Received: 3 October 2019 / Revised: 31 October 2020 / Accepted: 29 November 2020 / Published online: 3 January 2021

Abstract
Radioluminescent nuclear battery is an important representative type of indirect conversion in nuclear batteries. Design, fabrication, and performance optimization of such batteries have been studied in detail. The specific research contents including optimization of material parameters of fluorescent layers, fluorescent layer structure design, radioluminescent spectra regulation, and radioluminescence emission intensity enhancement. The electrical properties of nuclear batteries with different fluorescent layers were tested under beta particles and X-ray excitation. As the mass thickness of the fluorescent layer increases, the electrical performance parameters first increase and then decrease, and there is an optimal mass thickness. A series of ZnS:Cu phosphor layers with different structure geometric parameters were prepared by tape adhesion method. When the thickness of the phosphor layer is close to the radioactive particle range, a good output performance can be achieved. Moreover, the effect mechanism of nano-fluorescent materials has also been introduced to improve battery performance. $CsPbBr_3$ perovskite quantum dot thin film materials and their applications in the radioluminescent nuclear batteries have been studied. $CsPbBr_3$ can effectively enhance the spectral response coupling degree, and greatly improve the output power of the battery. Further, a novel type of radioluminescent material using CdSe/ZnS core–shell quantum dot coupled with Au nanoparticles was prepared. The results show that the nano-coupling system can indeed improve the luminescence emission intensity and battery output performance. This research work can provide a new direction for future space battery technology.

Keywords Nuclear battery · Radioluminescence · Performance optimization design · Space energy · Space exploration

1 Introduction

With the continuous extension of human exploration, the exploration of the space field is also facing more and more challenges, and power technology has become the main constraint [1]. The breakthrough in the development of battery application technology will definitely bring great impetus to the exploration. Nuclear batteries have attracted much attention due to their high energy density, long life, strong environmental adaptability, and stable work [2–4]. It is even considered by the space community to be an almost irreplaceable power supplier. A nuclear battery is a device that converts the energy of a radioisotope source into electrical energy. Different power batteries can display their own characteristics and can be well applied. High-powered nuclear batteries can be used as a power source to provide driving power to planetary probe vehicles. Low-power nuclear batteries can be used to independently supply small scientific instruments, micro-sensors and other electronic devices for space detection, or to trickle charge capacitors. Among them, the radioluminescent nuclear battery with high energy density, strong environmental applicability and miniaturization design can be an important branch in the development of new micro-energy [5].

The radioluminescent nuclear battery is a kind of indirect transducing battery, which mainly includes three modules of the excitation source, fluorescent layer and photovoltaic module, as shown in Fig. 1. The energy conversion process consists of three stages: radioisotope originating from spontaneous decay, radioluminescent and photovoltaic effect. So

✉ Xiaobin Tang
tangxiaobin@nuaa.edu.cn

Zhiheng Xu
xuzhiheng@nuaa.edu.cn

Yunpeng Liu
liuyp@nuaa.edu.cn

[1] Department of Nuclear Science and Technology, Nanjing University of Aeronautics and Astronautics, Nanjing 211106, China

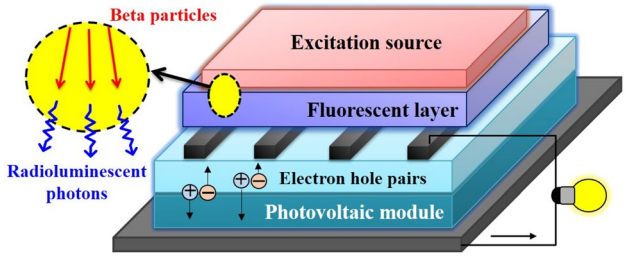

Fig. 1 Schematic diagram of radioluminescent nuclear battery device structure and working principle

far, a lot of research has been done on the materials used in batteries [6–8]. The morphology of radioactive sources and various hybrid radioluminescence sources have been investigated by some scholars [1, 9–11]. Based on the in-depth analysis of battery transduction mechanisms, the output performance can be improved by optimizing the way components are combined. Radioluminescent nuclear batteries with a wide range of materials can be developed into new nuclear energy sources, providing strong support for space exploration and space resource development. Based on the research of previous studies, this paper has carried out a series of researches on methods to optimize battery performance and experimentally tested its effective improvement effect.

2 Materials and Methods

The preparation of the fluorescent layer herein involves a variety of methods, such as physical sedimentation, tape adhesion, and spin-on film formation [1, 12, 13]. Among them, the physical sedimentation method can effectively control the thickness of the fluorescent layer, and the obtained fluorescent layer has good mechanical properties. The fluorescent layer prepared by the tape adhesion method is thin, has good flexibility, and can be bent into different shape structures. Spin-on film formation is mainly used here for the preparation of nano-fluorescent films. The quantum dot films involved in this paper are prepared by this method.

The fluorescent collection unit used in nuclear batteries is a gallium arsenide (GaAs) based photovoltaic module. The volt-ampere characteristic (*I*–*V*) curve of the radioluminescent nuclear battery was measured using a Keithley dual channel system source meter (Keithley Model 2636A, USA). All the fluorescent layer samples were placed in the dark environment for at least 24 h prior to electrical performance testing. During the test, the batteries were placed in an optically shielded dark box, and the positive and negative electrodes of the battery are connected to the fixture interface of the source meter, and the whole process avoids interference from external light or vibration. In addition, accidental errors generated during the test are minimized by multiple measurements.

3 Results and Discussion

3.1 Physical Parameters Optimization of the Fluorescent Layer

Three different types of fluorescent layers were prepared by acetone-assisted homogeneous precipitation technology with precise size control. A series of samples of different mass thicknesses were analyzed and tested, and the physical parameters are shown in Table 1. Different types of fluorescent layers are numbered 1–7 according to their mass thickness. These phosphors are representative of the traditional zinc sulfide matrix and rare earth phosphors. Among them, zinc sulfide copper-doped phosphors are selected from two different particle sizes to compare their performance for radioluminescent nuclear batteries. The area of different phosphor layers is consistent, and all are 3.0×3.0 cm^2. The beta sources with different particle energies and GaAs-based photovoltaic modules were used, and the corresponding electrical performance output was compared. The characteristic parameters of the beta sources used are shown in Table 2.

As illustrated in Fig. 2, the output power of the radioluminescent nuclear battery based on the above fluorescent

Table 2 Characteristic parameters of the beta sources

Beta sources	Half life (a)	Average energy (keV)	Activity density (mCi/cm^2)	Active area diameter (mm)
^{63}Ni	100.1	17.43	4.89	Φ25
^{147}Pm	2.62	61.93	2.23	Φ25

Table 1 Physical properties of three types of fluorescent layers

Phosphors	Particle size (μm)	Sample number and mass thickness (mg/cm^2)						
		1	2	3	4	5	6	7
ZnS:Cu-Large	38	7.59	8.03	13.22	25.33	25.81	38.48	51.11
ZnS:Cu-Small	7.4	4.89	10.20	12.31	20.40	31.11	31.29	36.47
Y_2O_2S:Eu	6.8	10.20	18.56	26.58	38.89	52.68	65.07	77.02

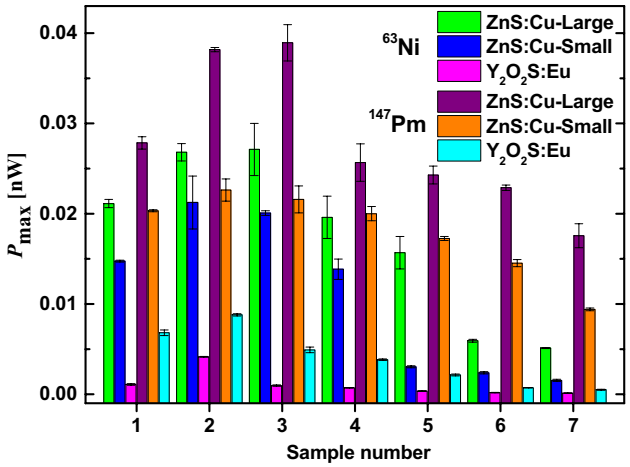

Fig. 2 Maximum power output of radioluminescent nuclear batteries consisting of different beta sources and different fluorescent layers. The sample number represents the different mass thicknesses of the fluorescent layers

layers was tested and extracted [14]. For each type of fluorescent layer, the maximum output power (P_{max}) of its corresponding nuclear battery exhibits a Gaussian distribution with increasing mass thickness. Comparing a certain type of fluorescent layer, it can be found that as the mass thickness increases, the battery power first rises and then falls, and there is a peak. The optimum mass thickness range for each battery varies. This optimum mass thickness is related to the fluorescent layer and excitation source used. The interesting phenomenon is that the performance of different fluorescent layers is consistent regardless of the relatively low energy ^{63}Ni or the relatively high energy ^{147}Pm source. Among them, the power of the ZnS:Cu-Large fluorescent layer-based nuclear battery is the largest, followed by the ZnS:Cu-Small fluorescent layer and the lowest is the Y_2O_2S:Eu fluorescent layer. The P_{max} of the nuclear batteries with the 2.23 mCi/cm^2 ^{147}Pm source was higher than that with the 4.89 mCi/cm^2 ^{63}Ni source. The experimental results show that under the premise of selecting the materials used in the nuclear battery, the battery output performance can be improved by optimizing the physical parameters of the fluorescent layer. The test results also show that ZnS:Cu is relatively performs better and is more suitable for radioluminescent nuclear battery preparation.

3.2 Structural Design Optimization of the Fluorescent Layer

Based on the above analysis results, a series of ZnS:Cu fluorescent layers of suitable thickness were obtained by a tape adhesion method. The phosphor layer used in this experiment consists of a ZnS:Cu phosphors layer and a transparent tape layer, both of which have thicknesses of 16 μm and 29 μm, respectively. 42 different V-shaped structure fluorescent layers were prepared and divided into model A and model B. The specific geometric parameters are shown in Table 3. The structural description of the fluorescent layer and part of the model diagram are shown in Fig. 3. The difference between Model A and Model B is whether the V-shaped structure is at the bottom or the top when it is aligned with the center of the excitation source. This difference reflects the extreme case where the relative positional shift of the fluorescent layer and the excitation source is maximized in the radioluminescent nuclear battery. The area of each phosphor layer that is ultimately projected to the bottom is 3.0×3.0 cm^2.

The output power of the radioluminescent nuclear battery based on the above different fluorescent layer structures is shown in Fig. 4 [15]. Under the excitation of the beta source of different energies, the trend of the curves is similar. Overall, the output power of the nuclear batteries based on 4.83 mCi/cm^2 ^{63}Ni source is greater than that of 1.36 mCi/cm^2 ^{147}Pm source. For the same excitation source, there are differences between the batteries based on models A and B, but they are generally not large. From the comparative analysis of the obtained results, it can be seen that the fluorescent layers with different angles and heights cause a large difference in the output performance of the nuclear battery. When one of the geometric parameters remains the same, the output power decreases as the other variable increases. That is, P_{max} decreases as the angle θ increases, as well as height h. In addition to this, the performance of the battery was measured when the fluorescent layer was a conventional plane structure. For the ^{63}Ni source, the single-layer plane structure exhibits good performance due to the relationship between the beta particle energy and the thickness of the fluorescent layer. However, for the ^{147}Pm source with a deeper particle penetration depth, when the geometric parameters are appropriate, the electrical output of the corresponding battery is significantly higher than that of the conventional

Table 3 Physical properties of three types of fluorescent layers

Geometric parameters	Values				
Height h (cm)	0.38	0.41	0.61	0.81	1.01
Bending angle θ (°)	30, 60, 90, 120, 150	30, 60, 90, 120, 150	30, 60, 90, 120	30, 60, 90, 120	30, 60, 90
Projected area (cm^2)	9	9	9	9	9

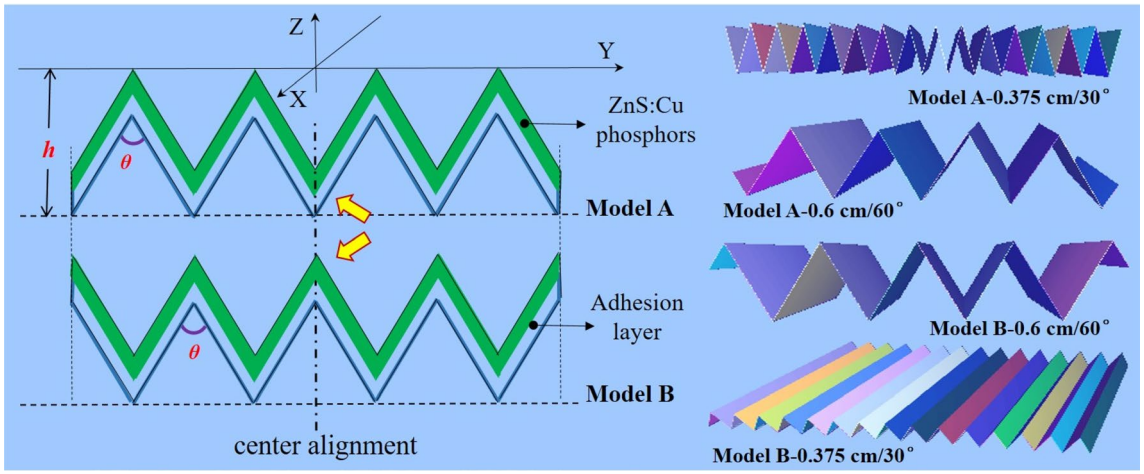

Fig. 3 The model of the V-groove fluorescent layers with geometrical structure parameters h and θ

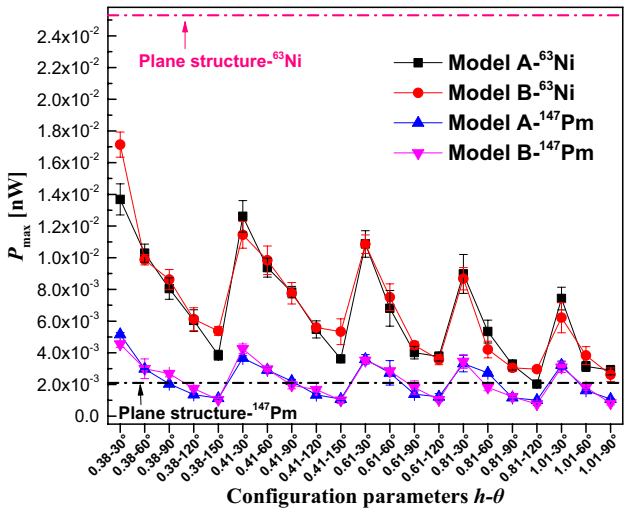

Fig. 4 Maximum output power of radioluminescent nuclear batteries with different configuration parameters of fluorescent layers

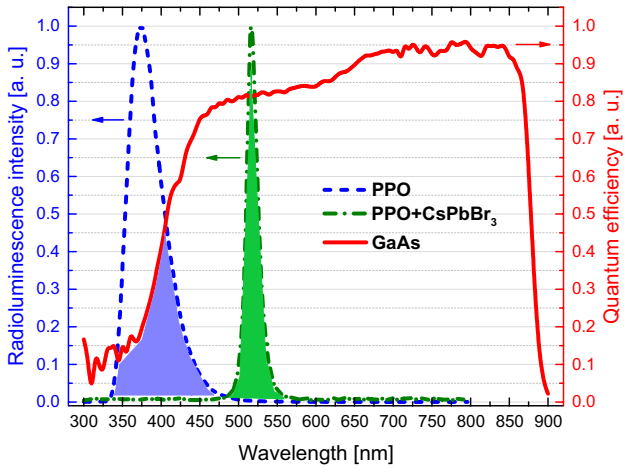

Fig. 5 Normalized radioluminescence emission spectra of PPO and PPO + $CsPbBr_3$, and normalized external quantum efficiency curves of single-junction GaAs photovoltaic modules

plane structure. It can be seen that for the determination of the fluorescent material and physical parameters used in the radioluminescent nuclear battery, the output performance can still be improved by changing its geometric parameters.

3.3 Regulation and Optimization of Radioluminescence Emission Spectra

At the same time, based on the previous research on battery performance optimization, it can be found that coupling the radioluminescence emission band of the fluorescent layer with the spectral response interval of the photovoltaic module as much as possible will facilitate the absorption and utilization of fluorescence, so as to improve the output power of the radioluminescent nuclear battery. For the all-inorganic bismuth-lead halide perovskite quantum dot fluorescent materials, their radioluminescence emission spectra can be adjusted by changing the halogen component and ratio. In addition, it also can affect other luminescent materials, and its emission wavelength is regulated by the Stokes shift effect [16, 17]. In this work, the $CsPbBr_3$ quantum dots with stable luminescence performance and good monochromaticity were taken as examples to study the influence of spectral control on the electrical output performance of the radioluminescent nuclear battery. Figure 5 shows the normalized radioluminescence spectra of separate poly phenylene oxide (PPO) and PPO mixed with $CsPbBr_3$ perovskite quantum dot. PPO is a common fluorescent material that is easy to process into a film. When the $CsPbBr_3$ perovskite quantum dots were added to the PPO, the peak position of the fluorescent material was significantly red-shifted, and the peak

emission wavelength was shifted from 375 to 517 nm. At the same time, the spectral response interval of GaAs can also be seen. After the regulation of the perovskite quantum dots, the emission spectrum is almost entirely within the response interval of the GaAs photovoltaic module, and the quantum efficiency is high.

As illustrated in Fig. 6, the *I–V* curves of the nuclear battery before and after spectral control using $CsPbBr_3$ under different X-ray tube parameters was presented. The tube current is fixed at 0.8 mA and the voltages are set to 30, 40, 50, and 60 kV, respectively. As the radiation intensity parameters of the X-ray excitation source increase, the output performance parameters of the radioluminescent nuclear batteries based on the "PPO" and "PPO + $CsPbBr_3$" fluorescent layers are gradually improved. The output power of the battery gradually increases as the tube voltage increases, and there is a positive correlation between them. After PPO is optically regulated by $CsPbBr_3$, the electrical output performance of the corresponding nuclear battery under the same excitation condition is significantly improved, and the larger the excitation parameter, the better the output performance of the battery. When the tube current of the X-ray tube is 0.8 mA and the tube voltage is 60 kV, the output power of the spectrum-optimized radioluminescent nuclear battery is increased by 1.96 times. It can be seen that the technical scheme of adjusting the radioluminescence emission spectra of the nano-fluorescent material to improve the output performance of the nuclear battery is effective. Moreover, the higher the coupling degree between the emission spectrum of the fluorescent layer and the spectral response interval of the photovoltaic module, the better the optimization of the output performance of the battery.

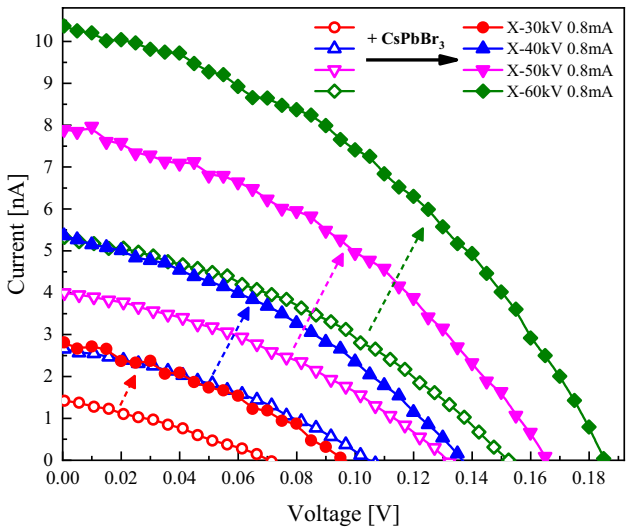

Fig. 6 *I–V* curves of radioluminescent nuclear batteries with PPO and PPO + $CsPbBr_3$ fluorescent material

3.4 Enhanced Radioluminescence Emission Intensity

On the basis of spectral adjustment using nano-fluorescent materials, some measures can also be taken to increase the radioluminescence intensity, thereby further making the final output of the nuclear battery higher. In this work, quantum dot nanotechnology and the surface plasmon resonance effects of noble metal nanometer systems are jointly introduced into nuclear batteries. In this experiment, oil-soluble CdSe/ZnS core–shell quantum dots with different concentrations (0.5, 1.0, and 4.0 mg/mL) and different emission wavelengths (480, 580, and 660 nm) were selected as experimental objects. The noble metal is selected from oil phase Au nanoparticles with a concentration of 50 μg/mL and a particle size of 15 nm. The *I–V* characteristic curves of the corresponding nuclear batteries are shown in Fig. 7, in which the amount of metal nanoparticles added in each sample is optimized.

According to the *I–V* curve of Fig. 7, the power parameters of the calculated battery are extracted, as shown in Fig. 8. For CdSe/ZnS core–shell quantum dots with different concentrations and emission wavelengths, the power-boosting effects are different. The P_{max} of the nuclear batteries with oil phase nano-coupling system can be increased from 1.01 to 15.48 times when the quantum dots are used alone. On the whole, the surface plasmon resonance enhancement effect based on metal nanoparticles can indeed enhance the emission intensity of radioluminescence. However, it is worth noting that the specific lifting effect is closely related to the physical parameters of the quantum dots used.

4 Conclusion

This paper aims to propose a series of performance improvement measures based on the energy conversion mechanism of the radioluminescent nuclear battery and verified that it is feasible. In this study, a series of effective methods to improve battery performance were proposed, mainly starting from the fluorescent layer that acts as a connecting link. By means of gradual and in-depth research, the physical parameters, structural design, fluorescence spectrum optimization and fluorescence emission enhancement of the fluorescence layer are studied in detail. Through these optimization measures, the output power of the radioluminescent nuclear battery can be increased up to 15.48 times before optimization. Although the above four optimization ideas are studied in depth and relative independently of each other, they can still be organically combined for a specific situation. Further, the quantum dot fluorescent material may be perovskite or cadmium quantum dot. The emission wavelength is changed by

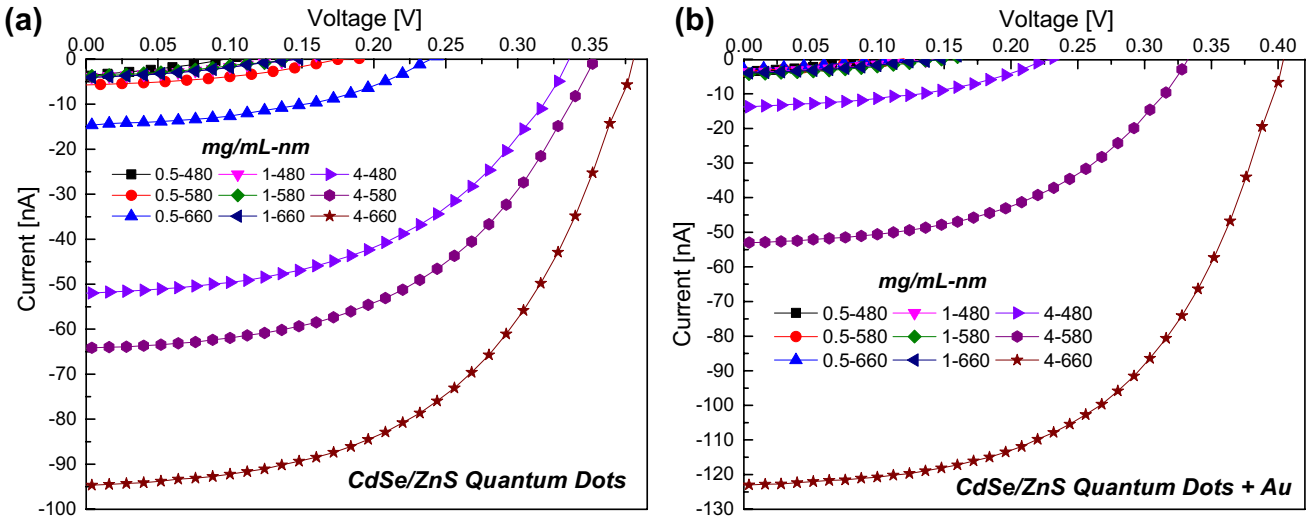

Fig. 7 *I–V* curves of radioluminescent nuclear batteries with **a** CdSe/ZnS and **b** CdSe/ZnS + Au fluorescent material

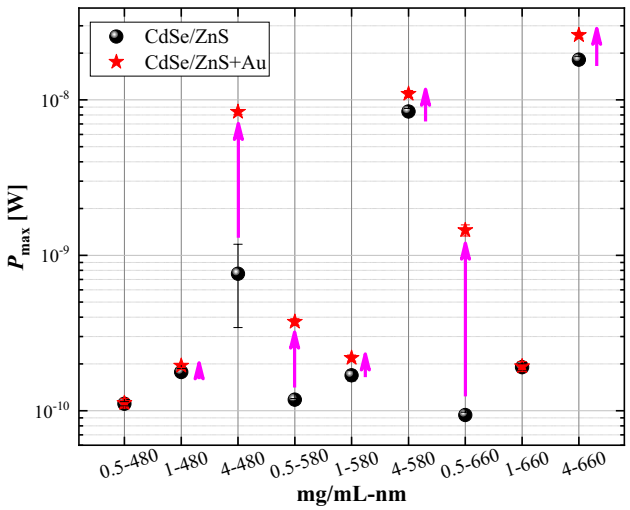

Fig. 8 Maximum output power of radioluminescent nuclear batteries with different nano-fluorescent material

its own preparation method and reaction conditions, and other fluorescent materials can also be affected to achieve spectral regulation. With the continuous development of space exploration, the demand for energy is more and more urgent, and the application of nuclear battery provides an effective solution. It is hoped that the mechanisms and effects involved in nuclear battery research will be helpful to the other fields, such as radiation detection, display devices and medical imaging.

Acknowledgements We acknowledge support from the National Natural Science Foundation of China (Grant Nos. 12005101 and 11675076), the Jiangsu Planned Projects for Postdoctoral Research Funds (Grant No. 1601139B), the Shanghai Aerospace Science and Technology Innovation Project (Grant No. SAST2016112), and the Fundamental Research Funds for the Central Universities (Grant No. NP2018462).

References

1. Bower K, Barbanel Y, Shreter Y et al (2002) Polymers, phosphors, and voltaics for radioisotope microbatteries. CRC Press, Boca Raton, pp 35–155
2. Lange R, Carroll W (2008) Review of recent advances of radioisotope power systems. Energ Convers Manage 49:393–401
3. Summerer L, Stephenson K (2011) Nuclear power sources: a key enabling technology for planetary exploration. Proc Inst Mech Eng Part G J Aerosp Eng 225:129–143
4. Nullmeyer B, Kwon J, Robertson J et al (2018) Self-healing effects in a semi-ordered liquid for stable electronic conversion of high-energy radiation. Sci Rep 8:12404
5. Xu Z, Tang X, Hong L et al (2014) Development of a beta radioluminescence nuclear battery. Nucl Sci Tech 25:040603
6. Bailey S, Wilt DM, Raffaelle RP et al (2005) Alpha-voltaic power source designs investigated. Res Technol 76–77
7. Sychov M, Kavetsky A, Yakubova G et al (2008) Alpha indirect conversion radioisotope power source. Appl Radiat Isotopes 66:173–177
8. Cress C, Redino C, Landi B et al (2008) Alpha-particle-induced luminescence of rare-earth-doped Y_2O_3 nanophosphors. J Solid State Chem 181:2041–2045
9. Schott R, Weaver C, Prelas M et al (2013) Photon intermediate direct energy conversion using a ^{90}Sr beta source. Nucl Tech 181:349–353
10. Lee H, Yim M (2017) Examination of scintillator-photovoltaic cell-based spent fuel radiation energy conversion for electricity generation. Prog Nucl Energ 94:46–54
11. Russo J, Litz M, Ray W II et al (2017) A radioluminescent nuclear battery using volumetric configuration: ^{63}Ni solution/ZnS:Cu, Al/InGaP. Appl Radiat Isotopes 130:66–74

12. Xu Z, Liu Y, Zhang Z et al (2018) Enhanced radioluminescent nuclear battery by optimizing structural design of the phosphor layer. Int J Energ Res 42:1729–1737
13. Xu Z, Tang X, Liu Y et al (2019) CsPbBr3 quantum dot films with high luminescence efficiency and irradiation stability for radioluminescent nuclear battery application. ACS Appl Mater Interface 11:14191–14199
14. Tang X, Xu Z, Liu Y et al (2015) Physical parameters of phosphor layers and their effects on the device properties of beta-radioluminescent nuclear batteries. Energy Technol 3:1121–1129
15. Xu Z, Tang X, Liu Y et al (2017) ZnS: Cu phosphor layers as energy conversion materials for nuclear batteries: a combined theoretical and experimental study of their geometric structure. Energy Technol 5:1638–1646
16. Chen W, Liu Y, Yuan Z et al (2017) X-ray radioluminescence effect of all-inorganic halide perovskite CsPbBr3 quantum dots. J Radioanal Nucl Chem 314:2327–2337
17. Chen W, Tang X, Liu Y et al (2018) Novel radioluminescent nuclear battery: spectral regulation of perovskite quantum dots. Int J Energ Res 42:2507–2517